Materials Research Bulletin 86 (2017) 72–79

Contents lists available at ScienceDirect

Materials Research Bulletin

journal homepage: www.elsevier.com/locate/matresbu

Synergetic effect of Li doping and Ag deposition for enhanced visible light photocatalytic performance of g-C_3N_4

Wenzhe Ma[a], Xiuying Wang[a,b,*], Feng Zhang[a], Xu Fei[b], Xiufang Zhang[a], Hongchao Ma[a], Xiaoli Dong[a,**]

[a] School of Light Industry and Chemical Engineering, Dalian Polytechnic University, #1 Qinggongyuan, Dalian 116034, PR China
[b] Instrumental Analysis Center, Dalian Polytechnic University, #1 Qinggongyuan, Dalian 116034, PR China

ARTICLE INFO

Article history:
Received 25 May 2016
Received in revised form 8 October 2016
Accepted 8 October 2016
Available online 11 October 2016

Keywords:
A. Composites
A. Semiconductors
B. Chemical synthesis
C. X-ray diffraction
D. Catalytic properties

ABSTRACT

g-C_3N_4 modified with Li doping and Ag deposition has been successfully prepared via a facile and cost-effective method. The composite presents the excellent photocatalytic performance for the degradation of Rhodamine B. The introduction of Li and Ag could effectively increase the absorbance in the visible light region, inhibit the recombination of photogenerated electron–hole pairs and improve the generation of reactive oxidation species. The synergetic effect between the Li doping and Ag deposition gives birth to the enhancement of photocatalytic activity of g-C_3N_4.

© 2016 Elsevier Ltd. All rights reserved.

1. Introduction

Solar-driven catalysis on semiconductors to produce clean chemical fuels and degrade organic pollutants is widely considered as the promising route to mitigate environmental issues [1–3]. Presently, the development of visible light-driven photocatalysts has been paid considerable attention. Among these visible light response photocatalysts currently available, graphitic carbon nitride (g-C_3N_4) has been the focus of intensive studies because of its abundance, high thermal stability, and good durability in various chemical environments [4–10]. However, low efficiency owing to the rapid recombination of photogenerated carriers limits the practical applications of g-C_3N_4.

Numerous strategies, including metal and non-metal doping [9–16], noble metal deposition [4,17,18], structural modification [19,20], and coupling with other semiconductors [5,8,21–24], have been attempted to address the aforementioned drawbacks. Doping with metal ions is considered as one of the most convenient and effective methods to modify electronic structures. Hu et al. [25,26] prepared alkali metal Na- and K-doped g-C_3N_4 and obviously improved their photocatalytic efficiency because of the enhanced optical absorption, increased surface area and accelerated charge carrier separation rate. In addition, several theoretical studies [27,28] report that doping Li into carbon nanotubes/graphene could also strongly affect their electronic structures. Zhu et al. [29] investigated the physical properties of Li-doped g-C_3N_4 monolayer by using first-principles density functional theory and proposed that the crystal structure of g-C_3N_4 monolayer was seriously distorted. Zhang et al. [30] reported that structural distortion could significantly modify the electronic structures of catalysts, resulting in efficient separation of photogenerated electron–hole pairs. Thus, according to Zhu's findings, doping Li into g-C_3N_4 could improve the activity of the photocatalyst. To the best of our knowledge, most of the available literatures concerning the effect of Li doping are based on theoretical research; virtually no research is based on experimental results.

g-C_3N_4 loaded with noble metal nanoparticles exhibits improved charge separation and transferability [17,18]. Besides, the surface plasmon resonance (SPR) effect of noble metal could also enhance the visible light response of g-C_3N_4 [17,18]. Up to now, g-C_3N_4 decorated with Ag nanoparticles has received marked attention because of its lower cost in comparison with that of platinum or gold. Zhu et al. [31] reported that g-C_3N_4 modified by highly dispersed Ag nanoparticles (~5.6 nm) exhibits enhanced photocatalytic activity for degrading organic pollutants under visible light irradiation. Although Ag nanoparticles have been widely used to further improve photocatalytic activity of the g-

---

* Corresponding author at: School of Light Industry and Chemical Engineering, Dalian Polytechnic University, #1 Qinggongyuan, Dalian, 116034, PR China.
** Corresponding author.
E-mail addresses: wang_xy@dlpu.edu.cn (X. Wang), dongxl@dlpu.edu.cn (X. Dong).

http://dx.doi.org/10.1016/j.materresbull.2016.10.011
0025-5408/© 2016 Elsevier Ltd. All rights reserved.

C_3N_4-based composites [32–35], relatively little attention has been paid to combining Ag deposition and metal doping as an approach.

On the basis of the above mentioned research progress, modification of g-C_3N_4 via Li doping as well as Ag deposition shows great potential in achieving highly effective photocatalysts. In this study, we report a facile, cost-effective method to synthesize Li-doped g-C_3N_4 for the first time. Our study reveals that the obtained sample exhibits excellent photocatalytic activity for Rhodamine B (RhB) degradation under visible light irradiation. After decoration with Ag nanoparticles, the catalyst exhibits significantly improved photocatalytic activity. The effects of doping Li^+ and Ag deposition on the structure and optical property, as well as the photocatalytic mechanism, are discussed in detail.

2. Experimental section

2.1. Preparation of Li-doped g-C_3N_4 (Li(x)–CN)

In a typical experiment, 1.0 g of melamine and designed amounts (0.05 g, 0.10 g, 0.15 g and 0.25 g) of lithium acetate were dispersed into 10 mL of deionized water under stirring. Then, the suspension was heated at 60 °C to evaporate the water and a solid product was obtained. Sequently, the solid product was heated at 550 °C for 4 h in a nitrogen atmosphere, and cooled down naturally to room temperature. Finally, the product was washed with deionized water several times, and then dried at 60 °C for a few hours. The obtained product was denoted as Li(*x*)–CN, where *x* stands for the amount of lithium acetate. Pristine g-C_3N_4 was prepared under the same conditions in the absence of lithium acetate.

2.2. Preparation of Ag/Li(0.15)–CN

Ag-loaded Li(0.15)–CN was prepared through photodeposition procedure [36]. 0.20 g of Li(0.15)–CN was dispersed in 50 mL of deionized water and 1 mL of 0.038 M $AgNO_3$ solution were then added slowly under stirring. The mixture was irradiated under 300 W Xe-lamp for 1 h with continuous magnetic stirring. After centrifugation, the sample was washed with deionized water and dried at 80 °C overnight to obtain Ag/Li(0.15)–CN. For comparison, Ag loaded g-C_3N_4 (Ag/CN) was prepared under the similar photodeposition procedure.

2.3. Characterization

The morphology of the samples was characterized by a scanning electron microscope (SEM, JEOL 7800F) and a transmission electron microscope (TEM, JEOL 2100). Powder X-ray diffraction (XRD) measurements were performed using a Shimadzu XRD-6100 diffractometer with Cu Kα radiation. N_2 adsorption–desorption measurements were performed on a JW-BK222 nitrogen adsorption analyzer. Photoluminescence (PL) spectra were recorded using a Perkin Elmer LS-55 spectrometer under 320 nm excitation. UV/visible diffuse reflection spectra (UV–vis DRS) were obtained over the range of 300–800 nm via a CARY 100 CONC spectrometer; here, $BaSO_4$ was used as the reflectance standard. X-ray photoelectron spectroscopy (XPS) was performed using a Thermo ESCA Lab250 spectrometer with Al K_α radiation. The Li and Ag contents in the obtained catalysts were determined by inductively coupled plasma atomic emission spectrometry (ICP-AES, Optima 8000).

2.4. Photocatalytic degradation of RhB

In a typical photocatalytic reaction, a 300 W Xe arc lamp (CEL-HXF300, Beijing China Education Au-light Co., Ltd.) with a UV–CUT filter to cut off light of wavelength $\lambda < 420$ nm was used as the irradiation source. 20 mg of photocatalysts was added to 50 mL of RhB solution with an initial concentration of 10 mg L^{-1}. Prior to photoreaction, the suspensions were magnetically stirred in darkness for 20 min to reach an adsorption-desorption equilibrium between the organic molecules and the catalyst surface. At an irradiation interval of every 10 min, the suspensions (3 mL) were collected and centrifuged to remove the photocatalyst particles. The RhB concentration was analyzed by UV–vis spectrophotometer (Shimadzu, UV-1600 pc) monitoring the absorption maximum at $\lambda_{max} = 554$ nm. To investigate the photocatalytic reaction mechanism, radical trapping experiments were performed under visible light irradiation ($\lambda > 420$ nm). The reaction condition was the photodegradation of RhB with the addition of isopropyl alcohol (IPA, 10 mmol/L), ammonium oxalate (AO, 6 mmol/L), and 1, 4-benzoquinone (BQ, 0.1 mmol/L) to scavenge the $^\bullet OH$, h^+, and $O_2^{\bullet -}$reactive species, respectively.

3. Results and discussion

Based on the results of ICP-AES analysis, the weight percentages of Li in Li(0.05)–CN, Li(0.10)–CN, Li(0.15)–CN and Li(0.25)–CN are around 0.36 wt%, 0.62 wt%, 1.04 wt% and 1.57 wt%, respectively. Fig. 1 shows the XRD patterns of pristine g-C_3N_4 and Li(*x*)–CN. The pristine g-C_3N_4 exhibits two peaks at 13.1° and 27.3°, which respectively correspond to the (100) and (002) crystal planes of g-C_3N_4 (JCPDS 87-1526). In contrast to pristine g-C_3N_4, gradual decreases in peak intensities at 13.1° of Li(*x*)–CN are observed with increasing Li content, which suggests that the crystal growth of g-C_3N_4 is inhibited by introduction of Li. This result is similar to those reports for g-C_3N_4 doped with Na and K [25,26]. No peaks for Li-related species are observed in the patterns of Li(*x*)–CN, demonstrating that Li^+ maybe doped into interstitial sites of in-planar g-C_3N_4. Unlike Na- and K- doped g-C_3N_4, no evident shift toward lower 2θ values is observed for all the Li(*x*)–CN samples. It could be attributed to the small ionic radii of Li^+, which is too small to enlarge the interplayer spacing of g-C_3N_4.

To confirm the presence of Li and identify the structure of the Li (*x*)–CN samples, XPS measurements were conducted. Fig. 2 depicts the high-resolution XPS spectra for Li 1*s*, C 1*s*, and N 1*s* of Li(0.15)–CN samples. Consistent with the Li species in LiN_3, the binding energy of Li 1*s* is observed at around 55.3 eV (Fig. 2a), indicating that Li^+ is probably inserted at interstitial position and stabilized in the electron-rich g-C_3N_4 structure by Li–N bond [37]. The high-resolution C 1*s* spectrum of g-C_3N_4 (Fig. 2b) displays two peaks at 284.6 and 288.3 eV, which could be assigned to C=C and N—C=N species, respectively [31]. Fig. 2c presents the high-resolution N 1*s*

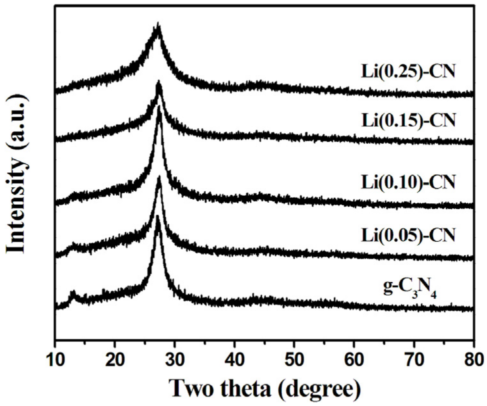

Fig. 1. XRD patterns of g-C_3N_4 and Li(*x*)–CN.

Download English Version:

https://daneshyari.com/en/article/5442287

Download Persian Version:

https://daneshyari.com/article/5442287

Daneshyari.com